Applications of advanced models to prediction of flatness defects in cold rolling of thin strips

Sami Abdelkhalek, Rebecca Nakhoul, Hamid Zahrouni, Pierre Montmitonnet, Nicolas Legrand, Michel Potier-Ferry

▶ **To cite this version:**

Sami Abdelkhalek, Rebecca Nakhoul, Hamid Zahrouni, Pierre Montmitonnet, Nicolas Legrand, et al.. Applications of advanced models to prediction of flatness defects in cold rolling of thin strips. 15th International Conference on "Advances in Materials and Processing Technologies - AMPT 2012, Sep 2012, Wollongong, Austria. hal-00724898

HAL Id: hal-00724898

https://hal-mines-paristech.archives-ouvertes.fr/hal-00724898

Submitted on 23 Aug 2012

HAL is a multi-disciplinary open access archive for the deposit and dissemination of scientific research documents, whether they are published or not. The documents may come from teaching and research institutions in France or abroad, or from public or private research centers.

L'archive ouverte pluridisciplinaire **HAL**, est destinée au dépôt et à la diffusion de documents scientifiques de niveau recherche, publiés ou non, émanant des établissements d'enseignement et de recherche français ou étrangers, des laboratoires publics ou privés.

Applications of advanced models to prediction of flatness defects in cold rolling of thin strips

S. Abdelkhalek [3], R. Nakhoul [2], H. Zahrouni [1], P. Montmitonnet [2*], N. Legrand [3], M. Potier-Ferry [1]

[1] LEM3, Université de Lorraine, UMR CNRS 7239, Metz, France,
[2] CEMEF, MINES ParisTech, UMR CNRS 7635, Sophia-Antipolis, France,
[3] ArcelorMittal Research Maizières, R&D Industrial Operations, Maizières-les-Metz, France

Flatness defects in thin strip cold rolling are a consequence of roll thermo-elastic deformation, from which heterogeneous strip plastic deformation results. When flatness defects manifest on line, buckling reorganizes the stress field in the pre- and post-bite areas. This might impact strain and stress fields *in* the bite, an effect which had been neglected. Two *coupled* Finite Element Method (FEM) approaches are presented here to examine to what extent such potential in-bite / out-of-bite feedback determines the in-bite fields and the flatness of the strip. Using both methods and comparing with the standard case where buckling is not accounted for, it has been shown[5] that (i) taking buckling into account results in a completely different stress field and fits correctly the measured on-line residual stress profile under tension (by "stress-meter rolls"); (ii) coupling buckling in the post-bite area and the rolling model, whatever the technique, changes little the in-bite fields. The models are applied here to several questions, namely the impact on flatness of heterogeneous temperature fields and of thinner edges, and the effect of friction on optimal setting of a flatness actuator, Work Roll Bending (WRB).

Keywords: Rolling, Thin Strips, Finite Element Method, Friction, Flatness Defect

1. INTRODUCTION

Due to rolls deforming elastically, the roll gap is not uniform in the width direction: strip reduction slightly depends on the width coordinate y (figure 1). The resulting residual stresses may be compressive locally in spite of the strip tension applied. In such a case, on-line manifested flatness defects (non developable, out-of-plane displacements) may occur for thin strips (Figure 1). They are due to (generally elastic) buckling, and form periodic waves (centre waves, edge waves…). If strip tension is high enough to maintain the strip flat (i.e. avoid buckling), residual stresses are present. When the strip tension is relaxed, or the sheet is cut, they may induce buckling and flatness defects. This is why the post-bite stress profile is called "latent flatness defects".

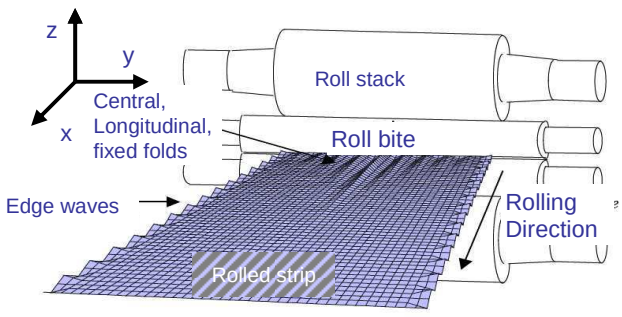

Fig. 1 Schematic view of flatness defects. Note reference frame.

* Author to whom correspondence should be addressed.

If defects are only latent, the stress field computed beyond the bite by e.g. a 3D FEM model should be correct. Buckling upon unloading the strip tension can then be dealt with in an uncoupled way, transferring the stress pattern computed by the rolling model into a buckling (shell e.g.) model. The latter then tells if the critical conditions for buckling are met, and in this case computes post-buckling wavelength and defect amplitude.

However, it is well known that buckling completely transforms stress fiel(ds the local stiffness drops dramatically). Therefore, if defects are manifested on-line as is most of the time the case for very thin sheets, the solution coming out of the 3D rolling FEM will be completely irrelevant beyond the bite. The question of the impact of this stress reorganization on the strains and stresses *within* the bite has been raised[12], with the conclusion that to the possible exception of temper-rolling, the feedback effect is very small: the post-bite stress rearrangement is screened by the immediate bite exit area were complex velocity profile changes take place in the elastic regime. The present paper examines other relevant questions, such as the set up of flatness actuators (WRB) or the effects or of usual model simplifications (isothermal versus thermally coupled).

2. BRIEF LITERATURE SURVEY

A number of uncoupled techniques have been presented in the literature. Bush et al.[1] and Fischer et al.[2] use the standard solution by Timoshenko and Woinovsky-Krieger[3] of von Karman's equations for a rectangular plate, assuming sinusoidal waves in both x and y directions. They extend it to the complex fields of strip rolling (buckling under residual stress). In Bush et al.[1] , only right/left symmetric waves are addressed. But real waves are often anti-symmetric, which Fischer et al.[2] allow by taking the transverse shape to be either an odd or an even polynomial in y, while remaining sinusoidal in the rolling direction.

Only the longitudinal stress (σ_{xx}) component is used in these papers. Moreover, the type of defect (centre or edge wave) is determined *a priori* from the shape of the stress profile, and *ad hoc* clamping boundary conditions are applied to get it in the end. Yukawa et al.[4] address more complete configurations using shell FEM, again with a non-coupled approach. The bifurcation point is detected as the load parameter making the second variation of the total elastic strain energy (or stiffness matrix) non definite positive. Post-buckling is computed by introducing a small defect corresponding to the mode, the load step being controlled by a modified Riks method.

Abdelkhalek et al.[5] maximize the load step and decrease the computational burden by managing the loading steps by the Asymptotic Numerical Method (ANM) (Zahrouni et al.[6], Boutyour et al.[7]). It consists in developing the solution (displacement and load parameter) in a power series with respect to a step length parameter, up to a truncation order *p*. This series is inserted in the non linear equations of the problem, the different orders are identified, giving *p* linear systems with the same stiffness matrix, and the right-hand sides of which are computed from the solutions at lower orders. They modeled both on-line shape (under strip tension) and relaxed shape, once strip tensions are relieved, whereas the previous papers dealt only with the latter.

Counhaye[8] was the first to question the decoupling of the rolling and the buckling model. Indeed, buckling sets a limit to the allowable compressive stresses: wherever buckling occurs, the loss of rigidity changes the stress locally and as the stress field must be re-equilibrated, global changes result. This thorough stress rearrangement on the one hand questions the stress fields obtained from the rolling models, on the other hand might have an impact even on in-bite stress and strain fields, or on roll deformation in strongly coupled cases. Therefore, Counhaye used an approach similar to Roddeman et al.[9], considering buckling as one more strain rate component, present only in the out-of-bite areas, to be added to the elastic / plastic strain rate decomposition. This extra strain rate represents the local shortening of a material segment when it becomes wavy due to buckling.

3. MODELS

3.1 Sheet Rolling model Lam3/Tec3

Based on the discussion presented above, the present paper introduces two algorithms coupling buckling and rolling models. The rolling model is Lam3/Tec3, a 3D strip / roll stack deformation software described in Hacquin et al.[10,11]. The strip deformation is dealt with by an implicit FEM with a velocity formulation using P1-discretisation on hexahedra. A *steady state* formulation based on streamlines is implemented. This requires integrating EVP constitutive equations along streamlines determined from the velocity field. A heterogeneous time step strategy called ELDTH has been introduced[10].

The roll stack thermo-elastic deformation model is based on advanced beam theory, Boussinesq solution of a half-space under general loading, and Hertz contact mechanics. This model is discretized by an influence function method, resulting in a system of equations in the roll rigid body displacement, contact line displacement field and contact pressure profiles at work roll / back-up roll and work roll / strip contact. This system is non-linear due to unknown contact lines. It is therefore solved by Newton-Raphson method.

Both strip and roll temperatures are computed by SUPG (Streamline-Upwind Petrov Galerkin) FE schemes. The strip model is 3D; the roll model is a combination of 2D (r,θ) and (r,z) models coordinated by an influence function technique.

3.2 Simple buckling model embedded in Lam3/Tec3

The model proposed by Counhaye[8] has been implemented in Lam3/Tec3 by Abdelkhalek[12]. Initially proposed within the membrane theory framework, it forbids the appearance of a negative stress: everywhere compression is about to occur, the structure buckles, bringing the stress back to almost zero by providing a stress-free alternative to *elastic* shortening of a material line. The following critical conditions are introduced:

$$\begin{aligned} \vec{n}_1.\sigma.\vec{n}_1 &= 0 \\ \vec{n}_2.\sigma.\vec{n}_2 &> 0 \\ \vec{n}_1.\sigma.\vec{n}_2 &= 0 \end{aligned} \quad (1)$$

where $\vec{n}_1$ and $\vec{n}_2$ are the directions of the principal Cauchy stress tensor in the buckled structure (hence the third equation). This means that when a tension is applied in a direction (here $\vec{n}_2$), the membrane is stiff; if the stress becomes negative, it gets slack and in fact, the corresponding stress is put to 0 (direction $\vec{n}_1$). The essence of the model consists in determining an extra deformation which elastically brings the stress in the buckled direction back to 0. It may be interpreted as the shortening of a material line due to buckling of the structure. This is more or less analogous to elastic-plastic decomposition, but is activated only out of the roll bite, i.e. where buckling *is allowed to* occur:

$$\Delta\varepsilon = \Delta\varepsilon^{el} + \Delta\varepsilon^{bu} \quad (2)$$

where $\Delta\varepsilon^{el}$ is the elastic and $\Delta\varepsilon^{bu}$ is the "buckling strain" increment. Plane stress is assumed out of bite.

The extra deformation representing buckling is computed in the principal axes, then transported to the reference frame. Let λ_i, i = I, II, be the principal components of this extra strain. It is deduced from σ_i, i = I, II as follows:

$$\lambda_i = \frac{\langle \sigma_i - \sigma_c \rangle}{E} \quad i = I, II \quad (4)$$

Moving back to the reference frame, the buckling strain increment is added to the global strain increment (u and v are the two in-plane incremental displacements, θ is the angle between principal and reference frames in the plane of the strip, ν is Poisson's ratio and E is Young's modulus):

$$\begin{aligned} \Delta\varepsilon_{11} &= \frac{\partial u}{\partial x} + \lambda_I \cos^2\theta + \lambda_{II} \sin^2\theta \\ \Delta\varepsilon_{22} &= \frac{\partial v}{\partial y} + \lambda_{II} \cos^2\theta + \lambda_I \sin^2\theta \\ \Delta\varepsilon_{12} &= \frac{1}{2}\left(\frac{\partial u}{\partial y} + \frac{\partial v}{\partial x}\right) + \left|\lambda_{II} - \lambda_I\right| \cos\theta \sin\theta \\ \Delta\varepsilon_{33} &= -\frac{\nu}{1-\nu}(\varepsilon_{11} + \varepsilon_{22}) \end{aligned} \quad (5)$$

This strain increment replaces the standard one fed into the module which solves the constitutive differential equations.

3.3 Staggered coupling of Lam3/Tec3 and ANM

The second model is the Asymptotic Numerical Method (ANM) described above in the non-coupled context. Here, it is coupled in a staggered scheme with Lam3/Tec3. A full Lam3/Tec3 simulation is run, until all iteration loops come to a converged solution. Then, the post-bite stress field is interpolated on the shell element mesh of the ANM buckling model. The six components of the stress field may be transferred, starting at the very edge of the bite, whereas all previous models used only the stabilized stress field, hundreds of mm after bite exit. It is quite important to involve this very complex bite vicinity area, where strong stress gradients exist, the impact of which must be clarified.

After this transfer step, a buckling and post-buckling analysis is performed by the ANM, changing the stress field in the post-bite part of the system. This might affect the exit line of the bite, which is the upstream edge of the shell mesh. This is considered as a novel boundary condition on the 3D FEM computation of strip and roll deformation. Its mesh is truncated at bite exit, and the abovementioned modified boundary stresses are applied. Lam3/Tec3 is run again in this new configuration, giving a slightly modified strip and roll deformation and stress pattern. Before going back to shell buckling, a new stress field must be computed in the post-bite area: this is done using another Lam3/Tec3 simulation, on a complete mesh this time, using only the last deformed roll stack (but with a "rigid stand" option). This puts an end to the corresponding iteration of the staggered scheme, and the whole procedure is repeated until convergence. In fact, coupling of bite and post-bite areas has been found weak, convergence is always reached at the third global iteration at most.

This is a somewhat complex, manual scheme, introducing possible information loss during transfers. The advantage is that the buckling model is highly powerful and reliable. Moreover, it is able to predict the shape, i.e. the wavelength and amplitude of any kind of flatness defect. Tthe previous one (section 3.2) can just predict the type and location of flatness defects, but suggests their severity indirectly and qualitatively only.

4. ROLLING OPERATION INVESTIGATED

4.1 Definition of rolls, material, strip dimensions

All examples shown hereafter refer to the same rolling pass, the last stand of a tinplate sheet mill, with very low thickness. All the characteristics are given in Table 1, together with the stress-strain curve:

$$\sigma_0 = (470.5 + 175.4.\bar{\varepsilon}) \times (1 - 0.45.\exp(-8.9\bar{\varepsilon})) - 175 \text{ (MPa)} \quad (6)$$

Table 1. Characteristics of investigated rolling pass.

Strip width	855 mm
Strip thickness (strip crown)	0.355 mm (4.81 %)
Exit thickness	0.252 mm
Rolling speed	22 m/s
Front / back tension	100 MPa / 170 MPa
Type of mill diameter WR diameter BUR Length WR Length BUR	4-high 555mm 1300mm 1400mm 1295mm
WR crown BUR crown	0.0322 % No crown
WR bending force / position	4.8 MN / y = 1010 mm
Screw force application	y = 1075 mm
Friction law	$\tau = 0,03 \times \sigma_n$
Young's mod. Poisson's ratio	E = 210 GPa ν = 0.3

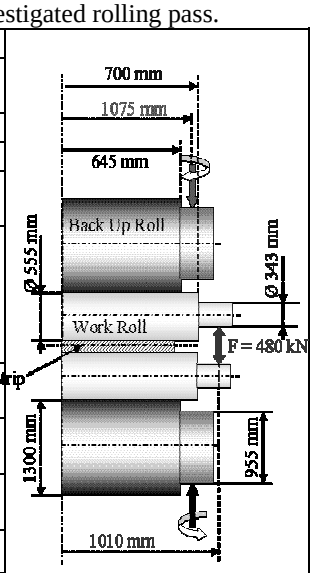

4.2 Impact of buckling being accounted for

With a reservation for very small reduction (temper-rolling), it has been found that this rearrangement of out-of-bite stress has significant impact neither on strain and stress fields in the bite, not on the roll loads and deformation[12]. Neglecting buckling is therefore licit if only the behaviour of the bite is to be described.

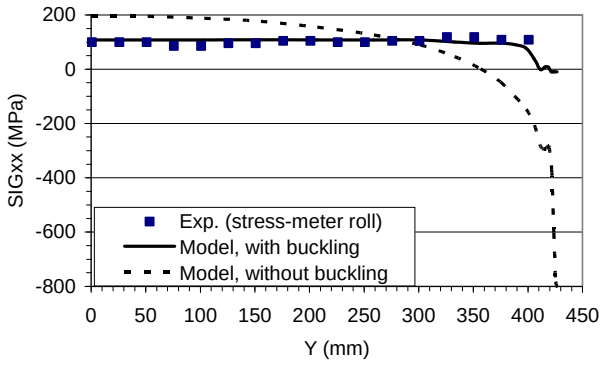

Fig. 2 Comparison of the experimental and numerical results (at shape-meter roll position).

However, the "residual" stress field in the strip is then completely wrong as shown in figure 2. The measurements (dots) show an almost flat stress profile (at the scale of the drawing). FEM without buckling gives enormous compressive stresses on the edge, due to a very large elongation gradient connected with roll flattening and the edge drop defect (see figure 3). This very high compressive stress is compensated for by a high tensile stress in the centre, since the resultant must be equal to the sheet tension force. When buckling is accounted for, the computed stress profile comes close to the experiments. More details can be found in a previous paper[12]. Therefore, for out-of-bite stress and comparisons with stress-meter measurements, accounting for buckling is essential, at least for thin strips.

5. FRICTION-SENSITIVE SETTING OF WRB

5.1 Impact of friction on roll deformation

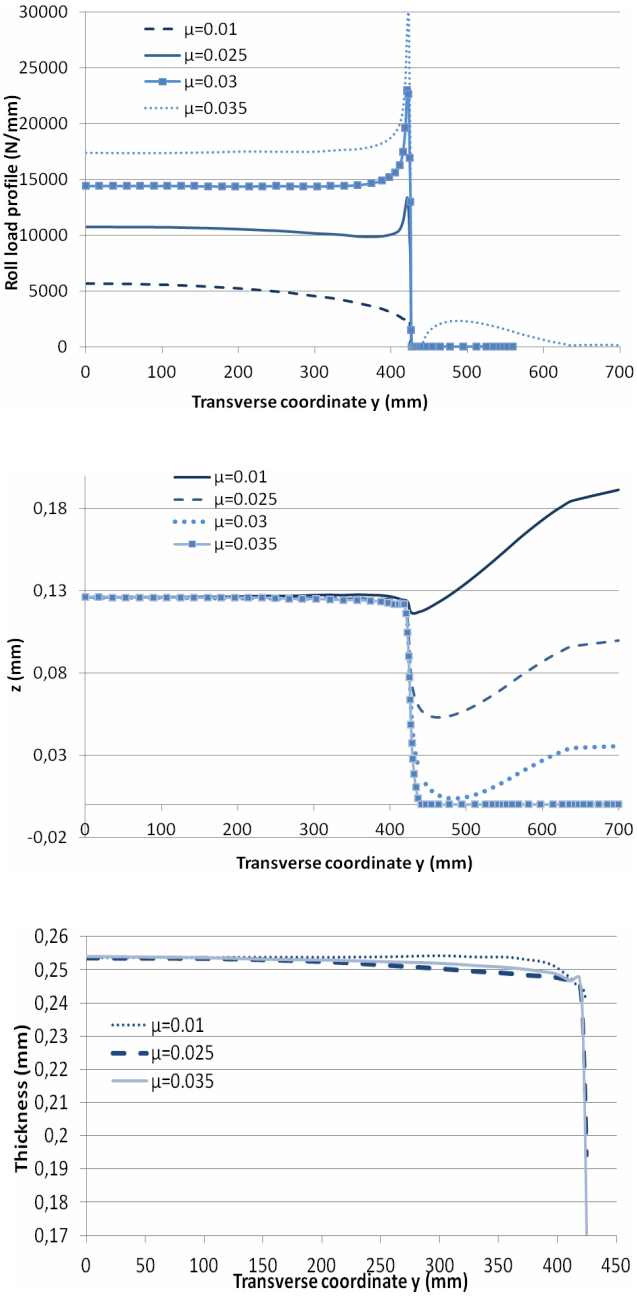

Fig. 3. The impact of friction on roll load transverse distribution (top), roll deformed profile (middle) and strip thickness profile (bottom). The WRB force is fixed here, 482 kN.

Work Roll Bending (WRB) is a typical sheet profile and flatness actuator: by applying a torque opposed to the contact stress moment, rolls are brought closer to their rest shape. This is a more flexible actuator than e.g. roll crown, which is chosen and fixed for a whole roll mounting. The WRB force can be controlled by monitoring the stress profile by the stress-meter roll, to answer variations in rolling conditions. Such variations often come from friction, which may fluctuate due to (i) progressive roll roughness wear from coil to coil and (ii) accelerations and decelerations at coil beginning and end. It has been proved to impact strip profile after cold rolling[13]; the effect of a parabolic variation of friction in the transverse direction has been evaluated[14]. It is therefore important to quantify the effects of such friction variations.

Figures 3 and 4 illustrate a parametric study whereby friction varies between $\mu = 0.01$ (slight skidding) and $\mu = 0.035$. The impact on roll deformation under a WRB force of -482 kN is first shown. Low friction gives a low rolling load, and moderate roll deformation. The shape of the WR generator therefore mainly corresponds to counter-bending by the WRB force. At $\mu = 0.035$, the rolling load is very high (compare the WR load profiles), so that roll kiss occurs (WRs touch each other on either sides of the strip). The resulting strip thickness profiles show small differences (a few µm), however very important in terms of residual stress and flatness. The latter are pictured in figure 4: $\mu = 0.01$ gives strong tension on edges and slack centre (wavy centre), whereas the stress profile is most flat when $\mu = 0.03$, leaving just a few mm of slack metal near the edges, with a probable small size wavy edge there.

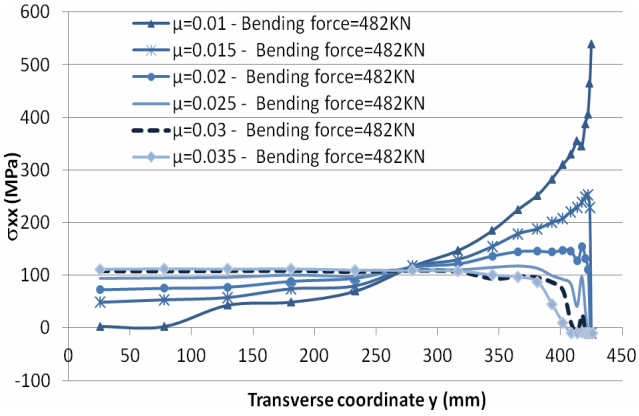

Fig. 4 The impact of friction and transverse profile of strip stress (latent flatness defect). The WRB force is fixed here, 482 kN.

5.2 Impact of work roll bending force at fixed µ

Now, the WRB force is varied at constant $\mu = 0.025$ (figure 5). The very high WRB force (900 kN) again gives a low, yet positive, stress in the centre, which will probably result in a wavy centre, at least after tension is cancelled. The most flat stress profile turns out to be for WRB = 350 kN.

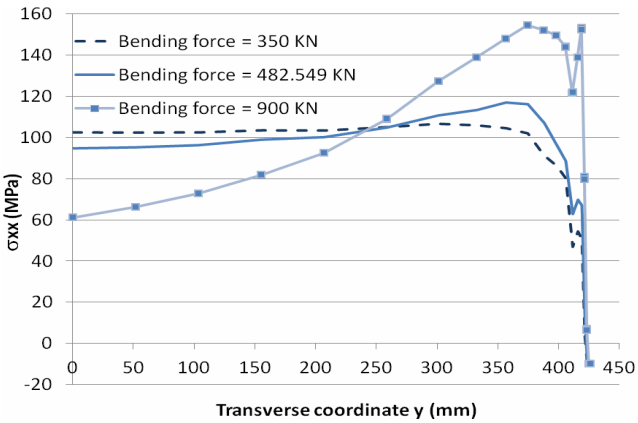

Fig. 5 The $\sigma_{xx}(y)$ stress profile for varying bending force and fixed friction coefficient ($\mu = 0.025$)

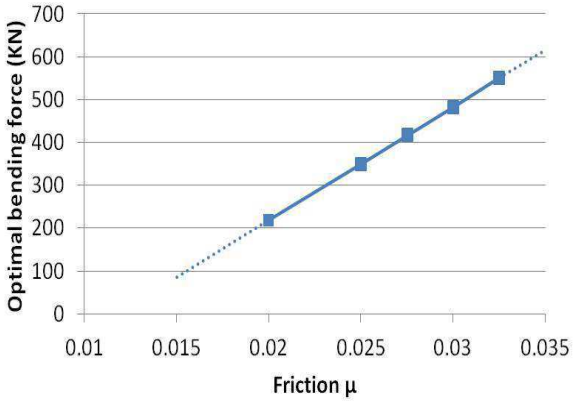

Fig. 6 The relationship between friction and optimal bending force

Finally, figure 6 summarizes the bending force found "optimal" for each value of the friction coefficient, i.e. giving the most flat stress profile "by eye". This graph gives an idea of how to pre-set the WRB force as a function of varying friction, in the present rolling operation of Table 1.

6. IMPACT OF TEMPERATURE FIELD

At bite exit, temperature is much larger at the edge than in the centre (figure 7), about 165°C versus 110°C. This is due to larger reduction and plastic heating (see figure 3). Due to the corresponding differential dilatation, the stress pattern could be affected. A series of simulations has therefore been run with the coupled buckling model of section 3.2, with roll temperature calculated at steady state (i.e. after a long rolling time).

The isothermal case is taken as a reference. In the second case, the strip is allowed to cool after bite exit under the effect of the strip cooling system, with $H_{cool} = 5$ kW.m^{-2}.K^{-1} for heat transfer coefficient (HTC); strip - roll contact is kept adiabatic ($H_{roll} = 0$). Temperature increases in the roll bite and slowly decays afterwards (remember 1 m ≈ 0.05 s).

In the third case, the roll - strip interface is represented by H_{roll} = 100 kW.m^{-2}.K^{-1}. The temperature increase is less in the bite, cooling is similar to the previous case. Finally, in the fourth case, H_{cool} = 5 kW.m^{-2}.K^{-1}, H_{roll} = 100 kW.m^{-2}.K^{-1}, but rolls are moreover cooled efficiently by water sprays, so that strip temperatures are significantly lower.

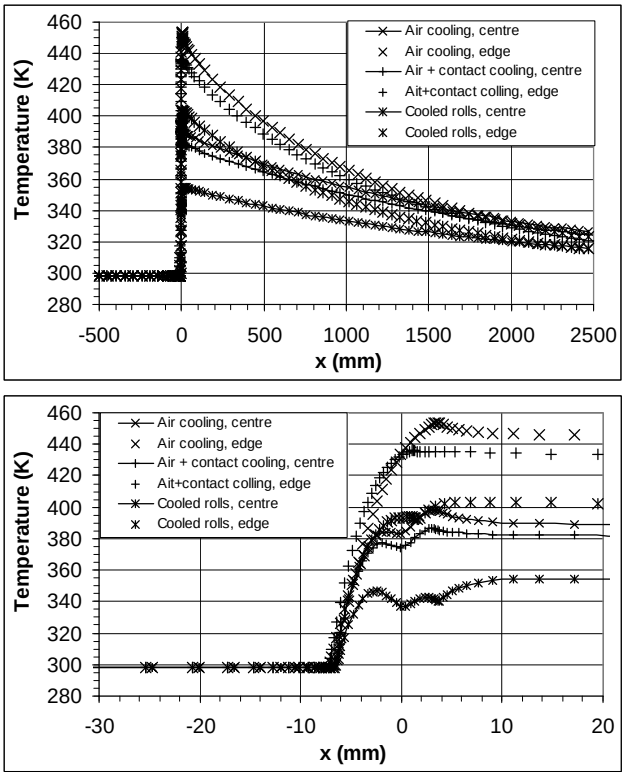

Fig. 7 Effect of thermal boundary conditions on central and edge longitudinal temperature profiles in the rolled strip. Top: long range post-bite evolution. Bottom: detail of plastic heating in the roll bite.

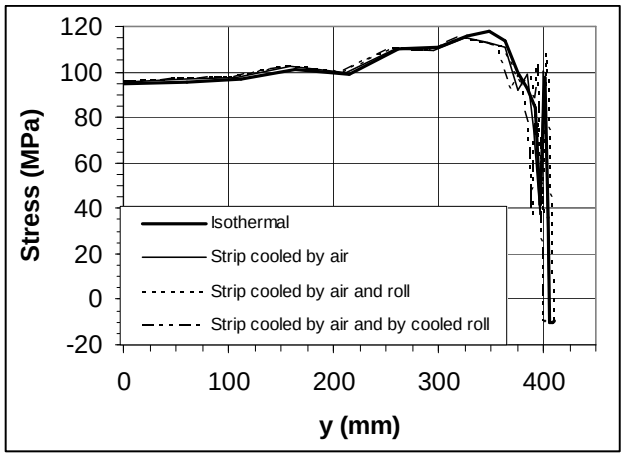

Fig. 8 Effect of all thermal boundary conditions on longitudinal stress transverse profile, $\sigma_{xx}(y)$.

However, the temperature difference between strip edge and centre is very similar in all 3 cases, 40 to 50°C. Figure 8 shows that these temperature differences, even in the isothermal case (T = 25°C everywhere), have negligible impact on the stress pattern once relaxed by edge buckling.

7. DOES THE EDGE DROP DEFECT ENHANCE WAVY EDGE FLATNESS DEFECTS?

As seen above, the edge is significantly thinner than the centre (in the case studied, central thickness is kept fixed at 0.252 mm by a supposedly perfect gauge control system, but it may drop to 0.18 mm on the edge). This means less rigidity against buckling of long edges as is the case here.

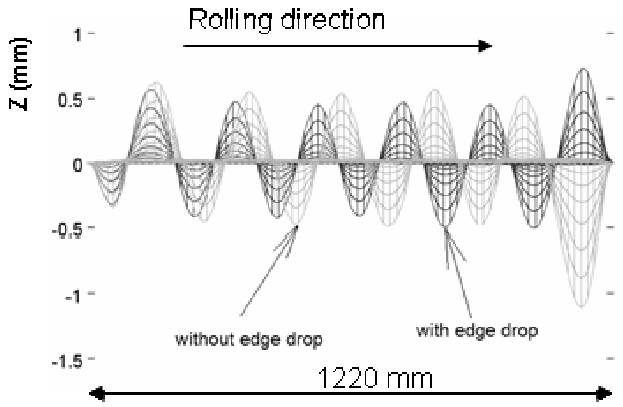

Fig. 9 Effect of edge thickness on relaxed strip shape. Black: the edge drop defect is taken into account; grey: the strip thickness is homogeneous.

To examine the effect of this, two simulations have been run with the ANM model (section 3.3), starting from the same residual stress map issued from the FEM rolling model – without buckling. The computation is isothermal, with μ = 0.25 and WRB force = 480 kN. 1200 mm of strip have been modeled by a shell mesh, with symmetry for the strip centre, a simply supported edge and a clamped bite exit. First, the 100 MPa strip tension is applied on the fourth side and buckling is calculated. Then the tension is eliminated progressively. The final strip geometry is pictured in figure 9. The wavelength is slightly shorter when the edge is more flexible, i.e. the geometric edge drop defect is taken into account. However, the two shapes are very similar, and it can be concluded that the effect is quite small even in this "favorable" case (low overall thickness, high edge drop defect).

8. CONCLUSION

Two different models of buckling leading to flatness defects have been presented. The first one (section 3.2) is very simple and deals with buckling at material point (or finite ele-

ment) level, which is questionable; but it is strongly coupled at constitutive equations level, which has been shown to be important for precise residual stress prediction. Its geometrical predictions are indirect and non-quantitative The second one (section 3.3) has the inverse characteristics: it is very precise and rigorous, it gives precisely and quantitatively the strip shape, but the rolling / buckling coupling is weaker and more tedious.

The main outcome of the present paper is to show that both models can be applied to practical questions concerning flatness in rolling. In-bite stress and strain are not affected by post-buckling stress rearrangement, but the residual stress is in case of manifested defects, which are almost always present on line with very thin strips. The results presented above suggest that for cold rolling, the heterogeneous temperature field does not change significantly the stress pattern, which is dominated by the rearrangement of the stress field as the elastic strain recovery takes place in the post-bite area.

It has been shown also here that friction has an impact on reduction profile through roll load distribution and roll deformation, and this strongly changes residual stress distribution when thin strips are dealt with. For a given work roll bending force, just changing friction may turn the strip shape from flat to wavy edge to wavy centre. Conversely, for each level of friction, an "optimal" WRB force is predicted.

Acknowledgments: The authors wish to thank the French National Research Agency (ANR) for its financial support, and the partners of the Platform Project for authorization to publish this work.

References and Notes

1. A. Bush, R. Nicholls, J. Tunstall, Stress levels for elastic buckling of rolled strip and plate. Ironm. Steelm. 28, 481-484 **(2001)**
2. F.D. Fisher, F.G. Rammerstorfer, N. Friedl, W. Wisser, Buckling phenomena related to rolling and levelling of sheet metal. Int. J. Mech. Sci. 42, 1887-1910 **(2000)**
3. S. Timoshenko, S. Woinovsky-Krieger, Theory of plates and shells, McGraw-Hill Book Co., New York **(1940)**
4. N. Yukawa, T. Ishikawa, Y. Tozawa, Numerical analysis of the shape of rolled strip, In Proc. NUMIFORM Conference, A. Samuelsson et al., Editors, p. 249-254 **(1986),** August 25-29, Gothenburg, Sweden
5. S. Abdelkhalek, H. Zahrouni, M. Potier-Ferry, P. Montmitonnet, N. Legrand, P. Buessler, Modélisation numérique du flambage des plaques minces et application au laminage. In Proc. (CD-ROM) CFM 2009, 6 p. **(2009)**, August 24-28, Marseille, France, in French
6. H. Zahrouni, B. Cochelin, M. Potier-Ferry, Computing finite rotations of shells by an Asymptotic-Numerical Method, Comp. Meth. Appl. Mech. Engg 175, 1-2, 71-85 **(1999)**
7. E.H. Boutyour, H. Zahrouni, M. Potier-Ferry, M. Boudi, Bifurcation points and bifurcated branches by an Asymptotic Numerical Method and Padé approximants. Int. J. Num. Meth. Engg, 60, 1987-2012 **(2004)**
8. C.Counhaye, Modélisation et contrôle industriel de la géométrie des aciers laminés à froid, PhD Thesis, Liège University **(2000)**, in French
9. D.G Roddeman, J. Drukker, C.W.J. Oomens, J.D. Janssen, The Wrinkling of Thin Membranes: Part I-Theory, ASME Trans. J. Appl. Mech. 54, 884-887 **(1987)**
10. A. Hacquin, P. Montmitonnet, J.P. Guilleraut, A steady state thermo-elastoviscoplastic finite element model of rolling with coupled thermo-elastic roll deformation, J. Mat. Proc. Tech. 60, 109-116 **(1998)**
11. A. Hacquin, P. Montmitonnet, J.P. Guilleraut, A 3D semi-analytical model of rolling stand deformation with finite element validation, Eur. J. Mech. A (Solids) 17, 1, 79-106 **(1998)**
12. S. Abdelkhalek, P. Montmitonnet, N. Legrand, P. Buessler, Coupled approach for flatness predictions in thin strip cold rolling, Int. J. Mech. Sci. 53, 651-675 **(2011)**
13. Z.Y. Jiang, A.K. Tieu, X.M. Zhang, C. Lu, W.H. Sun, Finite element simulation of cold rolling of thin strip, J. Mat. Proc. Tech. 140, 542–547 **(2003)**
14. Z.Y. Jiang, S.W. Xiong, A.K. Tieu, Q.J. Wang, Modelling of the effect of friction on cold strip rolling, J. Mat. Proc. Tech. 201, 85-90 **(2008)**